Optical Materials 41 (2015) 90–93

Contents lists available at ScienceDirect

Optical Materials

journal homepage: www.elsevier.com/locate/optmat

Studies of radiation defects in cerium, europium and terbium activated oxyfluoride glasses and glass ceramics

E. Elsts *, U. Rogulis, K. Bulindzs, K. Smits, A. Zolotarjovs, L. Trinkler, K. Kundzins

Institute of Solid State Physics, University of Latvia, 8 Kengaraga Street, Lv-1063 Riga, Latvia

ARTICLE INFO

Article history:
Available online 6 November 2014

Keywords:
Glass ceramics
Oxyfluorides
Optical absorption
TSL

ABSTRACT

Terbium, cerium and europium activated oxyfluoride glasses and glass ceramics have been studied by thermally stimulated luminescence (TSL) and optical absorption techniques after the X-ray irradiation. A creation of colour centres in oxyfluoride glass matrix and TSL peaks depending on the activator type were observed. LaF_3 and rare earth activators were analysed by SEM–EDS.

© 2014 Elsevier B.V. All rights reserved.

1. Introduction

Glass ceramics scintillators' advantages over single crystals are better uniformity and simplest production [1–3]. It would be a good material for applications where cheap and simple fabrication is more important than very high intensity or very short decay times.

First discovery of rare earth activator (Eu^{3+}) partitioning into LaF_3 crystals in the oxyfluoride glass–ceramic was published in a paper [4].

Many studies have been done of rare earth activator incorporation into LaF_3 crystals and its spectroscopy: europium [5], thulium [6], cerium and dysprosium [7], terbium [8] and other.

LaF_3 has relatively low phonon energies (300 cm^{-1}) [9,10], that reduce the quenching of the exited-states of lanthanide ions by lattice vibrations. LaF_3 shell does not change the luminescent properties of the luminescent ion [10]. Therefore, LaF_3 is a good host for rare-earth ions.

In our previous researches [11,12] we have studied terbium, cerium and europium activated oxyfluoride glasses and glass ceramics using various methods: differential thermal analysis, X-ray diffraction, cathodoluminescence and X-ray induced luminescence. X-ray induced luminescence showed that among the studied samples the most intense was a terbium activated glass ceramics sample – the integrated area of the spectral curve was about 10 times smaller than that of etalon sample CsI:Tl. Cathodoluminescence measurements showed that a cerium activated glass ceramics sample had the fastest decay times – average decay time was approximately 1.7 μs [12].

In this work, we have discussed creation of radiation defects in glass and glass ceramic samples after their X-ray irradiation. Experimental results have been obtained by thermally stimulated luminescence (TSL), optical absorption and scanning electron microscopy dispersive X-ray spectroscopy (SEM–EDS) techniques.

2. Experimental

2.1. Composition of samples

The investigated samples have the following molar composition: 48% SiO_2, 6% Al_2O_3, 24% Li_2O, 20% LaF_3 with different activators. The samples without activator hereinafter will be referred as SALL, those activated with 2% TbF_3 – SALL:Tb, 2% Eu_2O_3 – SALL:Eu and with 2% CeO_2 – SALL:Ce. After a heat treatment at 750–800 °C for 1 h glass ceramics have been formed [11].

2.2. Experimental equipment

Optical absorption spectra at room temperature were measured by the spectrometer Specord 210-2 using the integrating sphere with spectral range 380–1100 nm. The samples were X-ray irradiated at room temperature for 1 h.

Thermally stimulated luminescence spectra were measured by the Andor Shamrock B303-I spectrograph. For TSL measurements the samples were X-ray irradiated at liquid nitrogen temperature and then heated.

SEM (scanning electron microscopy) and EDS (energy dispersive X-ray spectroscopy) results were obtained by the SEM-FIB Tescan

* Corresponding author. Tel.: +371 29977814; fax: +371 67132778.
E-mail address: eelsts@cfi.lu.lv (E. Elsts).

http://dx.doi.org/10.1016/j.optmat.2014.10.042
0925-3467/© 2014 Elsevier B.V. All rights reserved.

Lyra equipped with Oxford Aztec spectrometer. Samples for SEM and EDS studies were cut and polished.

3. Results

3.1. Optical absorption for the SALL (non activated) glass and glass ceramics samples

Fig. 1 shows absorption spectra of the SALL sample before and after irradiation with X-rays. As the glass ceramic samples were not transparent, we used integrating sphere, which limits the minimum measurable wavelength to 380 nm. The glass ceramic sample has a broad absorption bands around 550 nm and 750 nm. After X-ray irradiation the glasses and glass ceramics have a higher absorption than before.

3.2. Activated SALL samples

Figs. 2 and 3 show absorption spectra of the glass and glass ceramics samples before and after X-ray irradiation, respectively. Generally the optical density of the activated glasses and glass ceramics after X-ray irradiation increases. All the activated glass ceramics (SALL:Eu, SALL:Ce, SALL:Tb) have higher absorption than the non activated glass ceramics (SALL) and glass samples. The SALL:Tb glass ceramics has the highest absorption among the investigated samples. We did not observe any new absorption bands in the SALL:Tb spectra, that would indicate to the formation of the same defects as in other samples.

Optical density of X-ray irradiated samples decreases with time after a heat treatment and defect concentration decreases. Absorption reduction after the heating is faster for the SALL:Tb than that of the SALL:Eu and the SALL:Ce glass ceramic samples.

Summarizing the results of the induced optical absorption, we have observed that very broad induced absorption bands could be created by the X-ray irradiation and that they are not very dependent from the activator type or from the presence of crystallites.

3.3. Thermally stimulated luminescence measurements

3.3.1. TSL for the SALL glass and glass for the SALL (non activated) samples

We performed measurements of TSL curves in the temperature range 77–350 K. Figs. 4 and 5 show that the SALL glass and the SALL glass ceramic TSL curves and spectra intensity of glass ceramic samples curves are about 50 times more intense than the intensities of the glass samples.

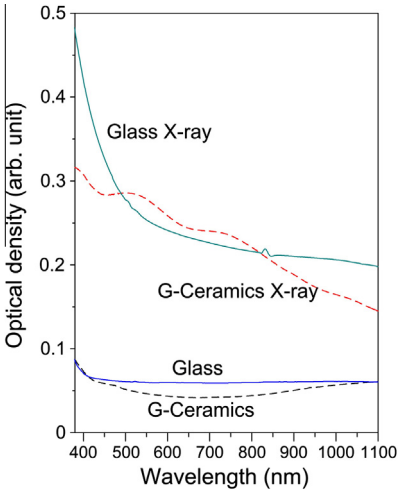

Fig. 1. Optical absorption spectra before and after irradiation with X-rays.

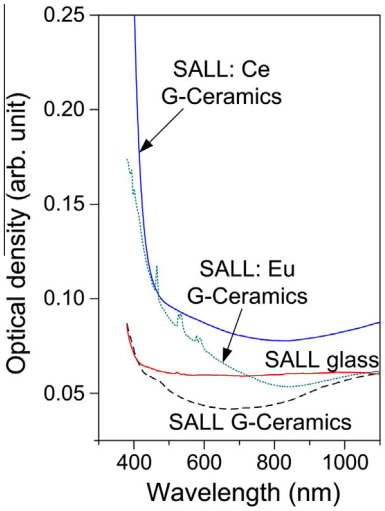

Fig. 2. Absorption spectra of the glass and glass ceramics samples before X-ray irradiation.

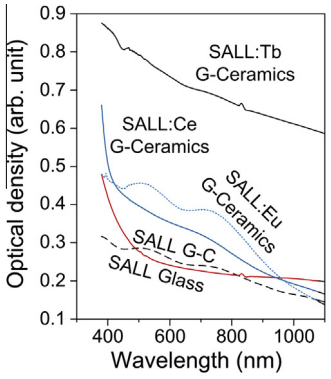

Fig. 3. Absorption spectra of the glass and glass ceramics samples after X-ray irradiation.

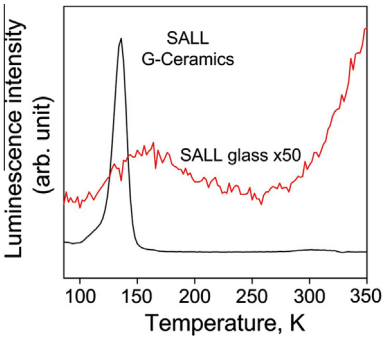

Fig. 4. TSL curves of the SALL glass and the SALL glass ceramic, measured at the luminescence wavelength 734 nm.

3.3.2. TSL for the SALL and activated glass ceramics

To show TSL curves and TSL luminescence spectra we selected one wavelength – 700 nm (Fig. 6) and one temperature – 140 K (Fig. 7) for all samples.

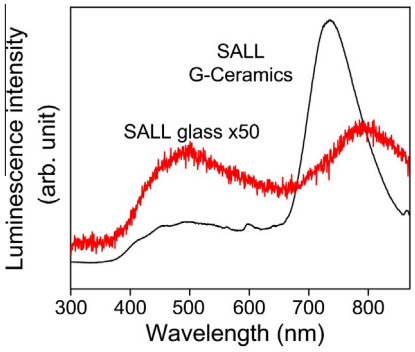

Fig. 5. TSL spectra of the SALL glass and the SALL glass ceramic, taken at temperature $T = 136$ K.

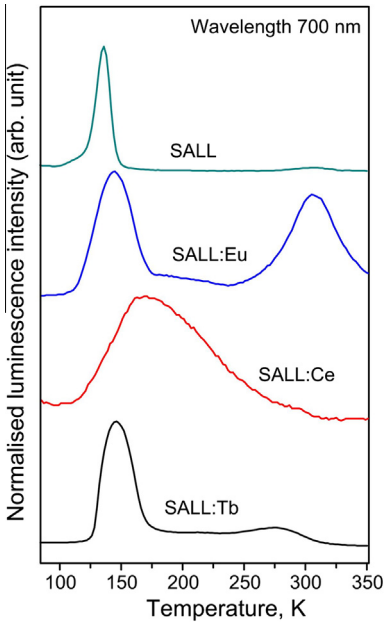

Fig. 6. TSL curves of SALL, SALL:Eu, SALL:Ce and SALL:Tb glass ceramic at different luminescence wavelengths.

Such wavelength and temperature are typical for high intensity luminescence region.

In all samples the TSL peaks (Fig. 6) were observed within the temperature range around 125–175 K. It indicates to some similarities of defects created in all the samples; however, the TSL peak at higher temperatures is strongly dependent on the activator and the measurement wavelength as well.

In the TSL (Fig. 7) spectrum of SALL:Tb we can see terbium energy level transitions: $^5D_3 \rightarrow {}^7F_J$ ($J = 6, 5, 4,3$) and $^5D_4 \rightarrow {}^7F_J$ ($J = 6, 5, 4, 3$). $^5D_4 \rightarrow {}^7F_J$ ($J = 6, 5, 4, 3$) transitions located at 490–620 nm which are much more intense.

The SALL:Ce has a wide spectral band at wavelength 350–575 nm corresponding to the electron transition $^2F_{5/2} \rightarrow {}^2F_{7/2}$ and additional band after 600 nm that could be attributed to the defect centres.

The SALL:Eu glass ceramics sample spectrum has peaks corresponding to energy level transitions $^5D_0 \rightarrow {}^7F_J$ ($J = 0,1,2,3,4$). We can observe also additional intense peak corresponding to the defect centres.

The SALL sample has a spectral band at the wavelength from of 675 nm, which could be attributed to a defect centre.

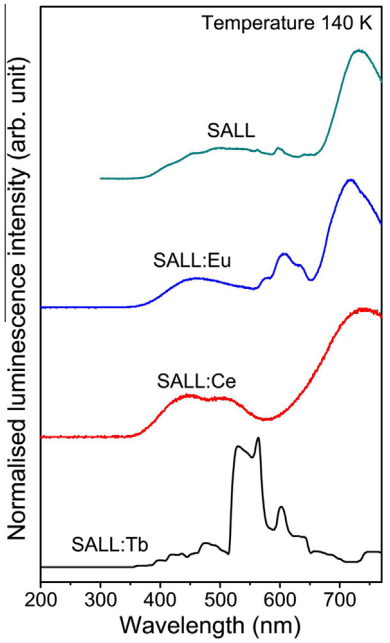

Fig. 7. TSL spectral distribution of SALL, SALL:Ce, SALL:Eu and SALL:Tb glass ceramic samples measured during the TSL process at 140 K.

For measurements of the TSL spectra monochromator slits were opened. To show terbium and europium band splitting we added X-ray luminescence spectra measured at room temperature (Fig. 8).

Although the measured peaks are not well resolved, the spectra clearly depend on the rare earth activator electron level transitions. We also observed other peaks which could be attributed to defect centres.

From all our TSL measurements, we may conclude, that the trap centres depend on the rare earth activators and, contrary to the induced absorption, these traps are mainly located in the fluoride crystallites.

3.4. Scanning electron microscopy

As reported earlier, XRD studies of our samples indicated presence of LaF_3 and $LiAlSiO_4$ crystalline phases [11]. Fig. 9 shows SEM and EDS results. In SEM–EDS mappings, a brighter colour indicates relatively higher concentration of element. SEM images show up to about 500 nm large areas with a higher concentration of the lanthanum and fluorine that agrees with obtained XRD data.

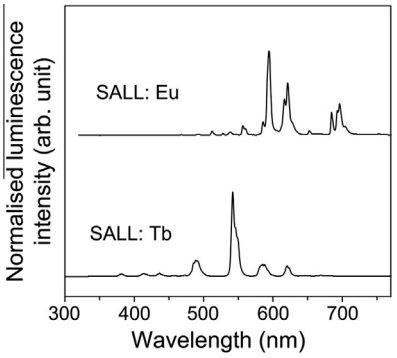

Fig. 8. X-ray stimulated luminescence spectra of SALL:Tb and SALL:Eu samples at room temperature.

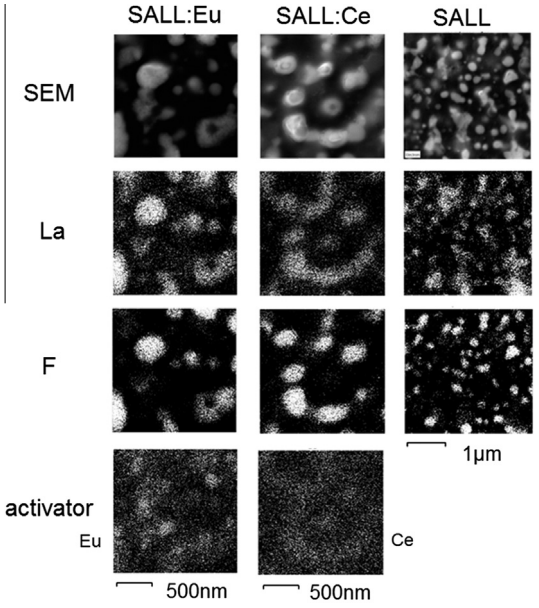

Fig. 9. Spatial location of the lanthanum, fluoride and activator (Eu, Ce) in the samples according the EDS measurements.

We observed that lanthanum and fluorine areas overlap. Rare earth activators are less distinctive than La and F due to their lower concentration. Europium and cerium ions are located in higher concentration inside and lower concentration outside La and F areas. We could not determine if any small part of europium ions have precipitated in pairs or even larger aggregates. EDS measurements have been performed on the surfaces of the samples. We could not obtain three dimensional LaF_3 image. Our previous studies showed luminescence intensity gain after heat treatment. We explained it with formation of LaF_3 crystallites [11].

Form SEM–EDS mappings (not shown) we have seen that $LiAlSiO_4$ forming elements Al, Si, O are overlapped as well, but we cannot determine lithium by this method.

For the discussion we found scientific research papers similar to ours.

Previously, $LiAlSiO_4$ (β-eucryptite, α-eucryptite) structure has been studied by NMR [13,14].

$LiAlSiO_4$ tetrahedra contain the following links: Si–O–Al, Al–O–Al, Si–O–Si and small amount of non bridged oxygen with negative charge.

Increase of absorption intensities has been observed after X-ray irradiation in Eu^{3+} activated $1Al_2O_3{\cdot}9SiO_2$ samples which are explained with hole creation [15].

X-ray irradiation of samples produces many oxygen deficiency centres that could be compensated by the activator ions.

Thermally stimulated luminescence (TSL) curves after X-ray irradiation have been observed in LaF_3:Tb^{3+} and other samples in temperature range 300–500 K and explained as an exciton upon recombination of the electron and hole [16].

So far we have not found an exact identification of the defect determining the induced optical absorption and TSL of our glasses and glass ceramics, further investigations are necessary.

4. Conclusions

Absorption spectra of samples after X-rays radiation show that creation of colour centres occurs mainly in the oxide glass matrix.

Trap centres observed by the thermoluminescence depend on the rare earth activators and are mainly created in the fluoride crystallites.

Scanning electron microscopy of the glass ceramics shows, that part of rare earth ions could be embedded in LaF_3 crystallites.

Acknowledgement

We thank the ESF (Project No. 2013/0046/1DP/1.1.1.2.0/13/APIA/VIAA/021) for financial support.

References

[1] C.L. Melcher, Nucl. Instrum. Methods Phys. Res. A 537 (2005) 6–14.
[2] J. Weber, J. Lumin. 100 (2002) 35–45.
[3] G. Blasse, Chem. Mater. 6 (1994) 1465–1475.
[4] M.J. Dejneka, J. Non-Cryst. Solids 239 (1998) 149–155.
[5] A.C. Yanes, J. Del-Castillo, J. Méndez-Ramos, V.D. Rodríguez, M.E. Torres, J. Arbiol, Opt. Mater. 29 (2007) 999–1003.
[6] A. de Pablos-Martín, D. Ristic, S. Bhattacharyya, Th. Höche, G.C. Mather, M.O. Ramírez, S. Soria, M. Ferrari, G.C. Righini, L.E. Bausá, A. Durán, M.J. Pascual, J. Am. Ceram. Soc. 96 (2013) 447–457.
[7] Q. Luo, X.S. Qiao, X.P. Fan, H. Yang, X.H. Zhang, S. Cui, L. Wang, G. Wang, J. Appl. Phys. 105 (2009) 043506.
[8] Z. Pan, K. James, Y. Cui, A. Burger, N. Cherepy, S.A. Payne, R. Mu, S.H. Morgan, Nucl. Instrum. Methods Phys. Res. A 594 (2008) 215–219.
[9] D. Chen, Y. Yu, P. Huang, Y. Wang, CrystEngComm 11 (2009) 1686–1690.
[10] P.R. Diamente, M. Raudsepp, F.C.J.M. van Veggel, Adv. Funct. Mater. 17 (2007) 363–368.
[11] U. Rogulis, E. Elsts, J. Jansons, A. Sarakovskis, G. Doke, A. Stunda, K. Kundzins, IEEE Trans. Nucl. Sci. 59 (2012) 2201–2206.
[12] U. Rogulis, E. Elsts, J. Jansons, A. Sarakovskis, G. Doke, A. Stunda, K. Smits, Radiat. Meas. 56 (2013) 120–123.
[13] S.K. Lee, J.F. Stebbins, J. Non-Cryst. Solids 270 (2000) 260–264.
[14] P. Daniels, C.A. Fyfe, Am. Mineral. 86 (2001) 279–283.
[15] M. Nogami, T. Ishikawa, Phys. Rev. B 63 (2001) 104205.
[16] W.J. Schipper, G. Blasse, J. Lumin. 59 (1994) 377–383.